Shear-thickening Polishing of inner raceway surface of bearing and suppression of edge effect

Luguang Guo
Xu Wang (wx382935877@163.com)
Zhejiang University of Technology https://orcid.org/0000-0002-1778-1064
Binghai Lyu
Linlin Cao
Yuechu Mao
Jinhu Wang
Hongyu Chen
Jiahuan Wang
Julong Yuan

Research Article

Keywords: shear-thickening polishing, inner surface, uniformity, high efficiency, bearing

Posted Date: April 7th, 2022

DOI: https://doi.org/10.21203/rs.3.rs-1506092/v1

Title Page

Shear-thickening Polishing of inner raceway surface of bearing and suppression of edge effect

Luguang Guo[a,b] Xu Wang[a,b*] Binghai Lyu[a,b] Linlin Cao[c] Yuechu Mao[a,b] Jinhu Wang[a,b] Hongyu Chen [a,b] Jiahuan Wang[a,b] Julong Yuan[a,b]

[a] *College of Mechanical Engineering, Zhejiang University of Technology, Hangzhou, China*

[b] *Ultra-Precision Machining Center, Key Laboratory of Special Purpose Equipment and Advanced Processing Technology, Ministry of Education and Zhejiang Province, Zhejiang University of Technology, Hangzhou, China*

[c] *Mechanical Engineering College, Beihua University, Jilin, China*

Title: Shear-thickening Polishing of inner raceway surface of bearing and suppression of edge effect

Author names and affiliations:

1. *Given name*: Luguang, *Family name*: Guo

Affiliations address: Ultra-Precision Machining Center, Key Laboratory of Special Purpose Equipment and Advanced Processing Technology, Ministry of Education and Zhejiang Province, Zhejiang University of Technology, Hangzhou, P.R. China, 310023

e-mail address: glg7127@163.com

2. *Given name*: Xu, *Family name*: Wang

Affiliations address: Ultra-Precision Machining Center, Key Laboratory of Special Purpose Equipment and Advanced Processing Technology, Ministry of Education and Zhejiang Province, Zhejiang University of Technology, Hangzhou, P.R. China, 310023

e-mail address: wx382935877@163.com

3. *Given name*: Binghai, *Family name*: Lyu

Affiliations address: Ultra-Precision Machining Center, Key Laboratory of Special Purpose Equipment and Advanced Processing Technology, Ministry of Education and Zhejiang Province, Zhejiang University of Technology, Hangzhou, P.R. China, 310023

e-mail address: icewater7812@126.com

4. *Given name*: Linlin, *Family name*: Cao

Affiliations address: Mechanical Engineering College, Beihua University, Jilin, P.R. China, 132021

e-mail address: caolinlin0626@126.com

5. *Given name:* Yuechu, *Family name:* Mao

Affiliations address: Ultra-Precision Machining Center, Key Laboratory of Special Purpose Equipment and Advanced Processing Technology, Ministry of Education and Zhejiang Province, Zhejiang University of Technology, Hangzhou, P.R. China, 310023

e-mail address: maoyuechu@126.com

6. *Given name:* Jinhu*, Family name:* Wang

Affiliations address: Ultra-Precision Machining Center, Key Laboratory of Special Purpose Equipment and Advanced Processing Technology, Ministry of Education and Zhejiang Province, Zhejiang University of Technology, Hangzhou, P.R. China, 310023

e-mail address: wangjinhu@zjut.edu.cn

7. Given name: Hongyu, *Family name:* Chen

Affiliations address: Ultra-Precision Machining Center, Key Laboratory of Special Purpose Equipment and Advanced Processing Technology, Ministry of Education and Zhejiang Province, Zhejiang University of Technology, Hangzhou, P.R. China, 310023

e-mail address: 15222918166@163.com

8. Given name: Jiahuan*, Family name:* Wang

Affiliations address: Ultra-Precision Machining Center, Key Laboratory of Special Purpose Equipment and Advanced Processing Technology, Ministry of Education and Zhejiang Province, Zhejiang University of Technology, Hangzhou, P.R. China, 310023

e-mail address: wangjiahuan1994@foxmail.com

9. Given name: Julong, *Family name:* Yuan

Affiliations address: Ultra-Precision Machining Center, Key Laboratory of Special Purpose Equipment and Advanced Processing Technology, Ministry of Education and Zhejiang Province, Zhejiang University of Technology, Hangzhou, P.R. China, 310023

e-mail address: jlyuan@zjut.edu.cn

Corresponding author:

Xu Wang, *e-mail address:* wx382935877@163.com*, T*el/fax: 86 057185290933

Shear-thickening Polishing of inner raceway surface of bearing and suppression of edge effect

Luguang Guo[a,b] Xu Wang[a,b*] Binghai Lyu[a,b] Linlin Cao[c] Yuechu Mao[a,b] Jinhu Wang[a,b] Hongyu Chen [a,b] Jiahuan Wang[a,b] Julong Yuan[a,b]

[a] *College of Mechanical Engineering, Zhejiang University of Technology, Hangzhou, China*

[b] *Ultra-Precision Machining Center, Key Laboratory of Special Purpose Equipment and Advanced Processing Technology, Ministry of Education and Zhejiang Province, Zhejiang University of Technology, Hangzhou, China*

[c] *Mechanical Engineering College, Beihua University, Jilin 132021, China*

Abstract: Shear-thickening polishing is a non-traditional finishing method that uses the shear thickening effect by impacting the non-Newtonian fluid over the machining surface. As a result, it forms a velocity gradient that increases viscosity sharply, producing a flexible fixed abrasive tool to remove the material. Shear-thickening polishing is applied for finishing the outer surface of the rotary workpiece in previous work. The material removal distribution on the inner surface is completely different from those on the outer surface due to the different structure. The thickened slurry tends to form a relatively dense boundary layer on the surface, resulting in a decrease in the polishing quality and efficiency. The present study investigates the effect of impact angle of slurry and polishing velocity on polishing quality to obtain the uniform surface morphology of the ring's inner surface by the shear-thickening polishing process. The inner raceway of the outer ring of the tapered roller bearing 30203 was taken as the machining object. The numerical material removal model of raceway surface was built according to the rheological performance of shear-thickening slurry. A mathematical geometric model is used to explore the real impact angle of slurry. The model was able to accurately predict the experimental conditions, and the results of the simulation were in good agreement with the model's predictions. In the fixture, a guide block was introduced to guide the flow of the slurry, ensuring consistent material removal across the whole surface. The optimal experimental results show that the average surface roughness measured by R_a reduces from 300 nm to 42.9 nm in 30 minutes, which further drops to 11.16 nm in 90 minutes with a variance of 0.58 nm^2. The conclusion could be drawn from the studies of this paper that uniform inner raceway surface of bearing is achievable through properly designed STP process.

keywords: shear-thickening polishing; inner surface; uniformity; high efficiency; bearing

1. Introduction

Surface quality requirements of key parts are becoming more and more stringent as industrial equipment develops, especially for work surfaces that influence part performance [1-4]. Being a core component of industrial equipment, bearing requires high integrity of surface morphology on raceway [5, 6]. The surface roughness not only affects the surface friction coefficient [7] but also extends the bearing life [8], meanwhile the raceway surface roughness has a significant impact on bearing noise and vibration under high-speed conditions [9]. However, the conventional raceway process by oilstone has a limitation of surface roughness of about 100 nm. Moreover, due to the forced plunge honing of abrasive particles under mechanical action, grinding heat and residual tensile stress generated by the machining are inevitable, leading to the generation of raceway surface degradation layer and limitation of surface quality.

Considering the inner concave surface characteristics of the inner raceway, it requires greater

skill to achieve a high surface quality than the outer raceway. Researchers have done extensive research on the application of ultra-precision machining technology for such inner surfaces. By using a magnetic polishing tool, Grover et al. [10, 11] reduced the surface roughness of an inner cylinder from 0.371 μm to 0.193 μm in 60 minutes, and that of a ferromagnetic workpiece from 360 nm to 90 nm in 100 minutes [12]. Zhen et al. [13] utilized a magnetic polishing tool with a rotating and linear coupled motion to machine the inner surface of a circular tube made of titanium alloy. After 2700 cycles, the surface roughness decreased by 24.7% to a minimum value of 0.197 μm. Umehara et al. [14] developed a special magnetically condensed material, which shows a magnetic fluid at high temperature, and can be solidified at room temperature. Umehara used a polishing tool made of this material to polish the brass and obtained a smooth surface that is 1/3 the original surface roughness. Zhang et al. [15, 16] polished the optical glass by five-axis equipment assisted with electrorheological polishing technique and found the reduction in surface roughness up to 10 nm within 30 minutes. However, neither magnetorheological nor electrorheological equipment/materials are exceptionally expensive. Meanwhile, during the magnetorheological/electrorheological polishing process, the slurry tends to concentrate at the entry of the polishing zone, leading to a decrease in polishing efficiency and quality [17].

Abrasive flow machining/polishing(AFM/AFP) has a relatively low cost and is widely used in ultra-precision machining of curved surfaces. Wu et al. [18] used AFM to processing the inner surface of small-diameter pipes, experiment results revealed that AFM could effectively reduce the roughness and remove surface defects. Zhang et al. [19] found that the thickness of oxide film affects polishing uniformity when CBN abrasive grains are mixed with AFM to process the hollow bearings. Zhao et al. [20, 21] numerically studied the inner surface processing mechanism by AFM and found that pressure at the inlet affects the intensity of turbulent flow; the stronger the intensity of turbulent flow, the higher the efficiency of processing. In order to polish the raceway of a large ring, Gao et al. [22] developed a fixture to guide the slurry's behavior and obtained the surface roughness of 0.1 μm. However, the AFM equipment requires good sealing and the processing efficiency was lower than the magnetorheological polishing method.

In summary, current flexible polishing technologies have various limitations when used for processing inner surfaces. Shear-thickening polishing (STP) method is a novel, flexible, contact polishing method that results in high removal rates and good surface quality. Li et al. [23] obtained surface roughness of 5.1 nm by polishing the Cr12Mo1V1 cylinder in 90 minutes. Lyu et al. [24] utilized brush-assisted STP for processing the cemented carbide inserts to obtain the surface roughness of 8.13 nm. Wang et al. [25] coupled the STP and electrochemical effect to polish the titanium alloy Ti-6Al-4V for reducing the surface roughness from 124 nm to 8.6 nm in 15 minutes. However, STP is a less explored technique for machining the inner surfaces. The flow field distribution while processing internal surfaces is completely different compared with external surface. When processing the outer surface, the solidified slurry can easily remove the material by relative movement with the workpiece surface pushed by potential flow, while processing the inner surface, it is difficult for the solidified slurry to slip over the surface. What's more, it tends to gather into a mass and adhere to the surface, depraving the processing efficiency and surface quality. Lyu et al. [26] developed a new method that uses a special wedge-shaped polishing tool to drive the slurry impacting surface, which could realize deterministic polishing of inner surfaces. This method has a low processing efficiency and needs a specific polishing tool according to the surface of the workpiece.

This paper attempts to realize the ultra-precision machining of the inner surface by the STP method. Taking the inner raceway of the 30203 bearing outer ring as the experimental object, a flow field constraint method was proposed to suppress boundary layer thickness by coupling the impact and flow behavior of the slurry in the paper. The study begins with the investigation of the influence of impact angles on polishing uniformity. It is followed by building a mathematical model to explore the true impact angle and analyze the flow field distribution in the polishing area through numerical analysis. The following sections deal with study of influence of impact velocity on polishing uniformity and remove rate through the numerical model developed above, use of a guide block to avoid the "edge effect" phenomenon, and realize the polishing uniformity on the whole curve surface. This paper provides a new technical approach for the precision polishing of inner raceway surface of bearing.

2. Experiment details

The principle of the ring's STP process is shown in Figure 1. The ring is fixed by a special fixture driven by the motor to rotate around its center. The shaft of the motor is inclined at an angle of $(\frac{\pi}{2}-\alpha)°$ from the horizontal plane. At the same time, the polishing disc rotates around at an angular speed ω, which drives the polishing liquid to rotate and impact the surface of the workpiece. The outer circle and the end face of the ring are protected by fixtures and polyurethane tapes to prevent them from being polished.

The thickened slurry adheres to the outer surface can easily peeled off by the potential flow with the rotation of the workpiece, which causing relative motion between thickened slurry and workpiece surface so that to remove material. In contrast, the flow field distribution of the slurry is closer to that of the pipeline flow when polishing the inner surface. As shown in Figure 2(a), when the velocity vector of the slurry is parallel to the wall, the adhered slurry is not easily removed by the potential flow. The thickness of the boundary layer $\delta(l)$ increases with the length of the wall, leading the effective length of the abrasive particles l is limited in the inlet area, and the material removal process is difficult and varies from point to point. As shown in Figure 2(b), when the potential flow impact the surface with a suitable incident angle, the normal velocity component can effectively reduce the thickness of the boundary layer, resulting the adapted effective length of the abrasive particles l' (l' ? l). The paper attempted to reduce the thickness of the boundary layer on the inner surface by adjusting the incident angle and impact velocity of the slurry, so as to realize high efficient and uniform polishing result of inner raceway of bearing.

Figure 3 shows the multi-axis STP machine as experiment platform. The slurry is formulated with deionized water (DI Water) and high hydroxyl polymer as thickening phase in a certain proportion to form a shear thickening liquid, and alumina abrasive particles are mixed as the polishing medium. The rest of the processing parameters are shown in Table 1. The material removal rate was measured by precision balance MSA225S-CE (Sartorius, Germany). As shown in Figure 4, the surface roughness of the ring was measured at starting point, middle point, and end point of the rolling contact surface of the roller-raceway by using a Taylor surface profiler (Form Talysurf i-Series 1) under the actual working conditions of the ring. The bevel angle β of the ring section was 12.5°. The microscopic surface morphology of the raceway was observed by an optical 3D surface

profiler (SuperView W1 midway) and a 3D microscope (VHX-S650E) with a super-high magnifying lens.

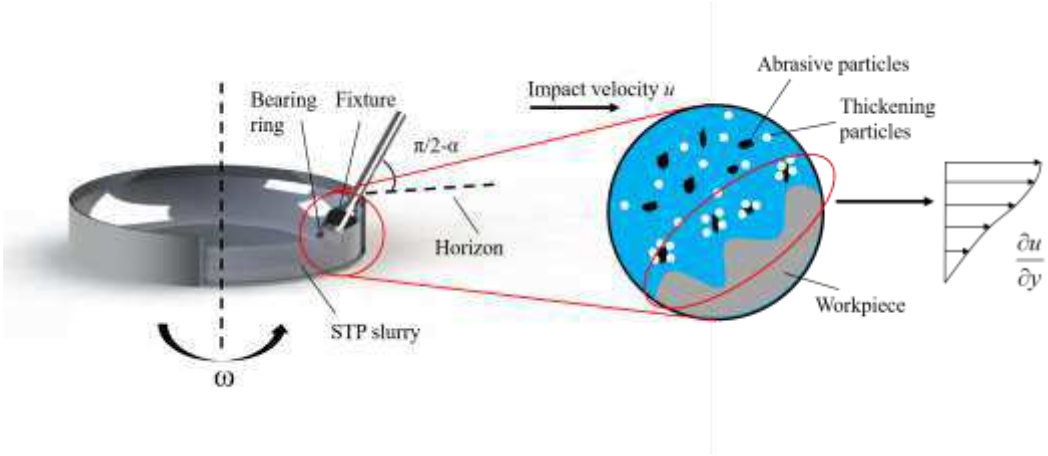

Figure 1 The principle of STP process machining bearing ring

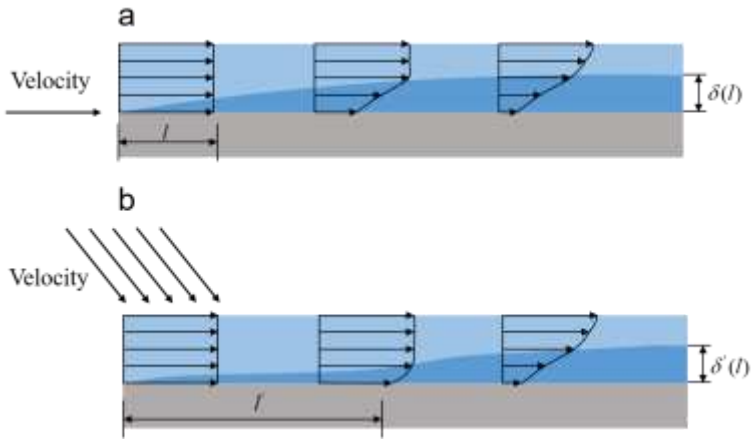

Figure 2 Evolution of boundary layer thickness under the action of velocity vector

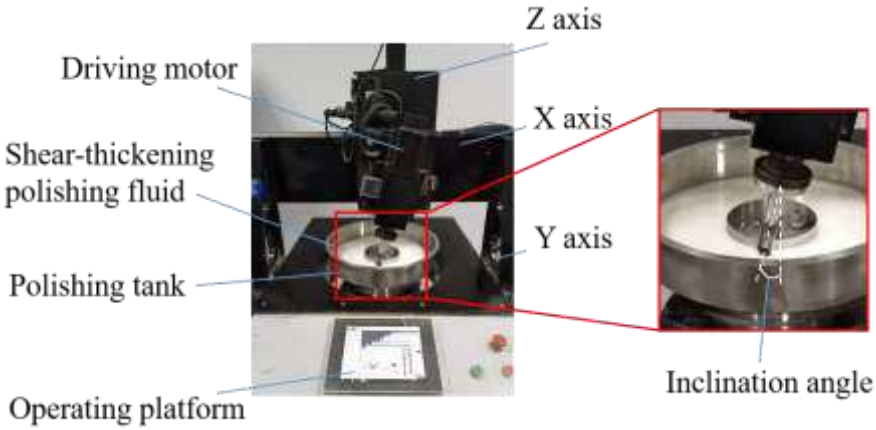

Figure 3 Multi-axis STP machine tool

Table 1 Experimental process parameter

Process parameter	Value
abrasive concentration (wt%)	5
abrasive particle size (μm)	5
polishing time (min)	30
rotation speed of the ring (rpm)	10
inclination angle of polishing shaft (°)	-12.5, 0, 12.5, 25, 37.5, 50, 62.5
rotation speed of polishing plate (rpm)	47, 60, 73, 86, 100

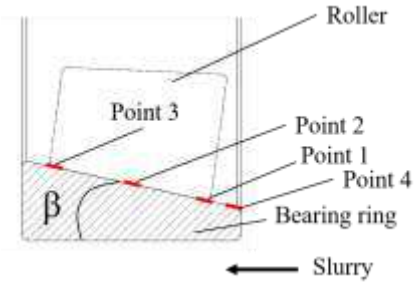

Figure 4 The position of the measuring points

3. Results and discussion

3.1. The effect of impact angle on polishing uniformity

3.1.1. Morphology variation and polishing uniformity with different inclination angles

Figure 5 shows the raceway surface morphology after polishing for 30 minutes duration under the inclination angle of 0°. As seen in the Figure, a small portion at the entrance has been finished by STP, while the remaining surface shows the grinding morphology. By processing the datum as shown in Equation 1, the micro-profile curve of the raceway surface can be obtained.

As shown in Figure 5(a), the peak corresponds to the surface micro-morphology formed by grinding, which easily breaks the lubricating film, causing load stress concentration and increasing the risk of fatigue failure. For the bearing raceways, the smooth surface helps retain lubricant thus improving the lubricating properties of the raceway interface. Figure 5(b) shows the profile curve and microscopic morphology of the raceway after being polished by STP. The microscopic profile curve is rounded at the corner, which improves frictional and wear performance, as the convex part smoothly joins the concave part [27]. To compare the degree of smoothness of raceway profile curves polished by STP, the uniformity of the polishing results can be qualitatively estimated.

$$x_i' = x_i + i \cdot \frac{x_N - x_0}{N}, i \subset (0, \mathrm{N}) \qquad \text{Equation 1}$$

where， x_i' is the calculated value of feature points' position, x_i is the initial value of feature

points' position, N is the total number of feature points.

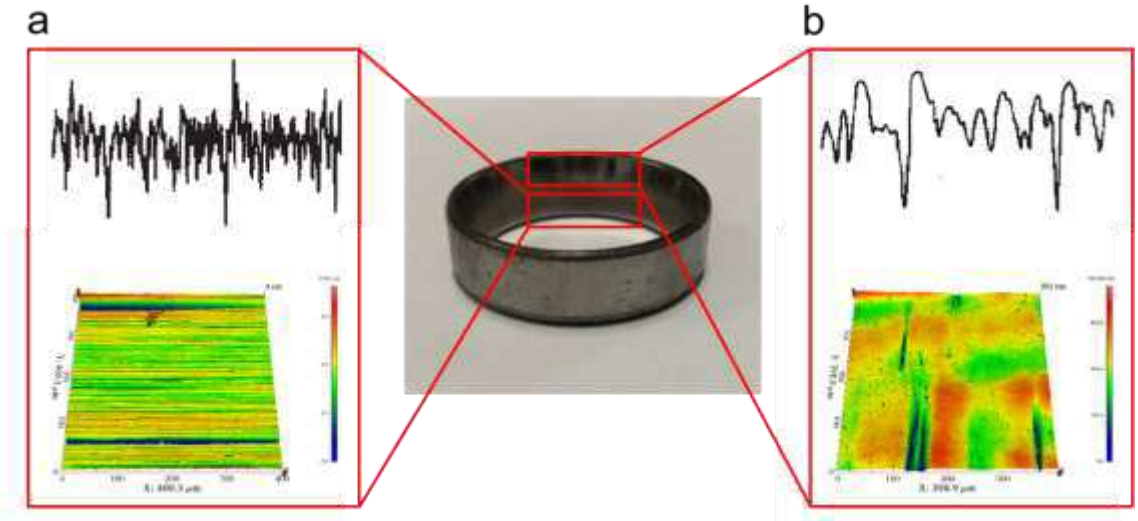

Figure 5 Profile curves and surface micro-morphology formed by different finishing methods：(a) after grinding；(b) after STP

STP experiments were carried out on the raceway for different inclination angles. The inclination angle refers to the fixed angle between the axis of rotation of the workpiece and the horizontal plane, which is $(\frac{\pi}{2}-\alpha)$ shown in Figure 1.

The polishing results are shown in Figure 6. For inclination angle of -12.5°, the surface morphology observes no significant changes and the roughness does not decrease; at 0°, the roughness decreases significantly only at the entry region and the morphology of the remaining area remains unchanged, which illustrates that shear-thickening effect diminishes; the overall surface roughness decreases significantly at inclination angles of 12.5° and 25°, however, the surface profile is relatively smoother at an inclination angle of 25°. Further increase in inclination angle brings uneven surface characteristics, which is an indicator of poor polishing quality. From the above experimental results, the best polishing outcome using the STP process is seen at a 25° inclination angle for a 30203 bearing ring raceway.

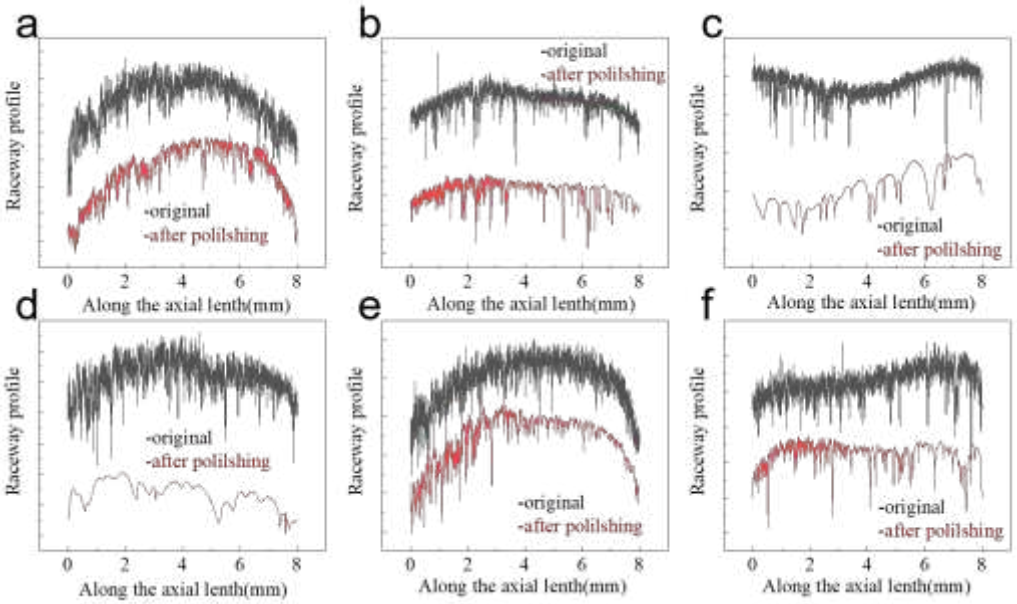

Figure 6 Comparison of profile curves at different inclination angles for 30 minutes duration: (a)-12.5°; (b)0°; (c)12.5°; (d)25°; (e)37.5°; (f)50°

3.1.2. The geometric model of impact angle

Figure 1 does not reflect the true impact angle due to processing conditions, so it is necessary to establish an accurate mathematical model in order to determine the true impact angle.

Figure 7 shows the geometric model of the ring during the STP process. The flow trajectory of the slurry was observed by fixing the ring as shown in Figure 7(a). The red area is the polishing trace, which has a large entrance and a small exit and slopes upward along the wall of the ring. The coordinate system and geometric symbols are set as shown in Figure 7(b)&(c). Assuming the true impact angle is θ, the midpoint of the entrance trajectory is marked as A and the midpoint of the trajectory at the exit is B.

AO_1 is the line joining point A and the center of the inlet circle O_1, and BO_2 is the line joining point B and the center of the outlet circle O_2. The angle between AO_1 and the vertical plane O_1O_2O is $2\theta_1$, and the angle between BO_2 and the vertical plane O_1O_2O is $2\theta_2$. The coordinates of points A and B can be obtained as follows:

$$\text{point A:}\begin{cases} x = 2r_1\sin^2\theta_1\cos\alpha \\ y = -r_1\sin(2\theta_1) \\ z = 2r_1\sin^2\theta_1\sin\alpha \end{cases},$$

$$\text{point B:}\begin{cases} x = (b\tan\beta + \dfrac{b}{\tan\alpha} + r_2(1-\cos(2\theta_2)))\cos\alpha - \dfrac{b}{\sin\alpha} \\ y = -r_2\sin(2\theta_2) \\ z = (b\tan\beta + \dfrac{b}{\tan\alpha} + r_2(1-\cos(2\theta_2)))\sin\alpha \end{cases},$$

where r_1 is the circular radius of the inlet circle, r_2 is the circular radius of the outlet circle, and the oblique angle of the ring section is β=12.5° as shown in Figure 4. The true impact angles of slurry can be obtained by using the cosine value of the angle between the vector $\overrightarrow{AB}$ and x-axis.

Table 2 shows the corresponding relationship between the inclination angle of the fixture and the true impact angle. It is worth noting that the ring is not processed at -12.5°, so it does not appear in the table.

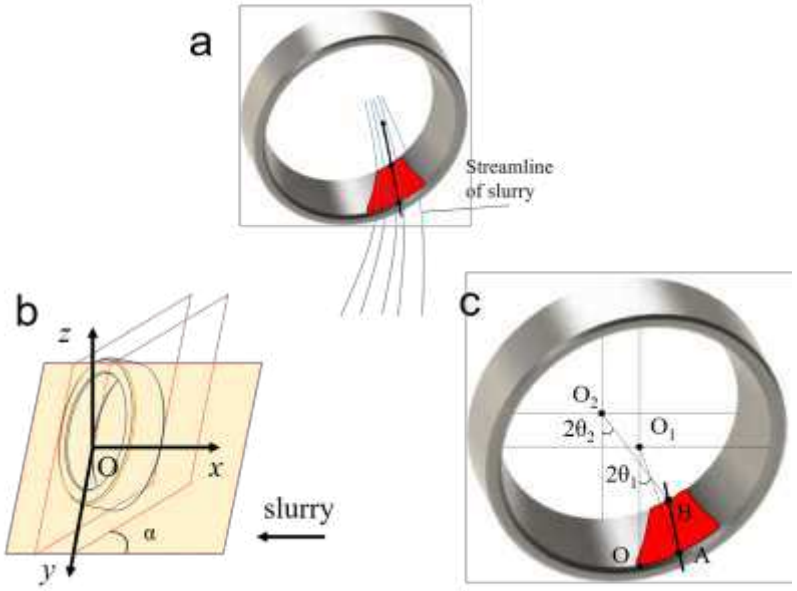

Figure 7 (a) Streamline trajectory of slurry；(b) Coordinate system；(c) Geometric parametric model

Table 2 The corresponding relationship between $(\frac{\pi}{2}-\alpha)$ and θ

the inclination angle of fixture (π/2-α)(°)	the true impact angle θ(°)
0	29.2022
12.5	31.5894
25	45.1626
37.5	69.9863
50	77.8310

3.1.3. Distribution of material remove

The flow through the channel is assumed to be a rectilinear flow, and thus it can be simplified as a 2D model. The model is shown in Figure 8: The gray area shows the cross-section of the outer ring of the 30203 bearing. The shear-thickening slurry enters the flow field from the left inlet and the outlets are set to pressure outlets with zero Gaussian pressure. Other simulation parameters are shown in Table 3[23], where λ is the viscosity thickening coefficient and n is the viscosity index of the shear-thickening slurry.

According to the Preston removal function, MRR (material removal rate) = K.P.v, which reveals that MRR is closely related to polishing pressure and relative motion speed. Thus, the

normalized equivalent of the P.v is used to evaluate the MRR of the STP process.

Figure 9 shows the evolution of pressure and velocity on the raceway surface profile under different impact angles. At different angles, the distribution has the same tendency to decrease followed by stabilization. According to Figure 9, the pressure and velocity changes at 19° can be divided into three zones. The zone1 is the initial contact area between slurry and ring shows a large decrease in pressure and velocity. However, the average P.v value remains the highest, which leads to a higher removal efficiency. The pressure and velocity changes tend to level off in zone2, resulting in good polishing consistency. Zone3 shows a significant decrease in pressure while velocity increases, however, the P.v value does not change much as opposed to zone2.

The results obtained from the preliminary analysis of the simulations are shown in Figure 11. Using an impact angle of 45-60° will provide the highest P.v on the ring surface, as well as the best removal efficiency and polishing quality. In general, this is consistent with the experimental data from the previous section.

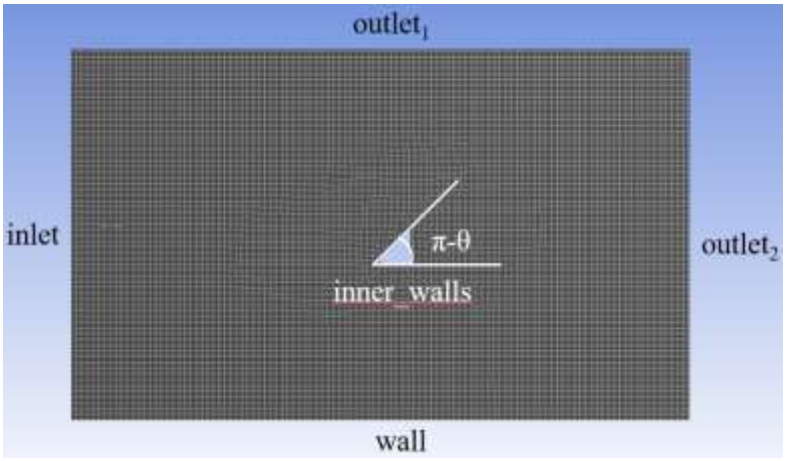

Figure 8 2D simulation model

Table 3 Simulation parameters

CFD parameters	Value
velocity of slurry($m.s^{-1}$)	1.3
λ	0.62
n	1.5

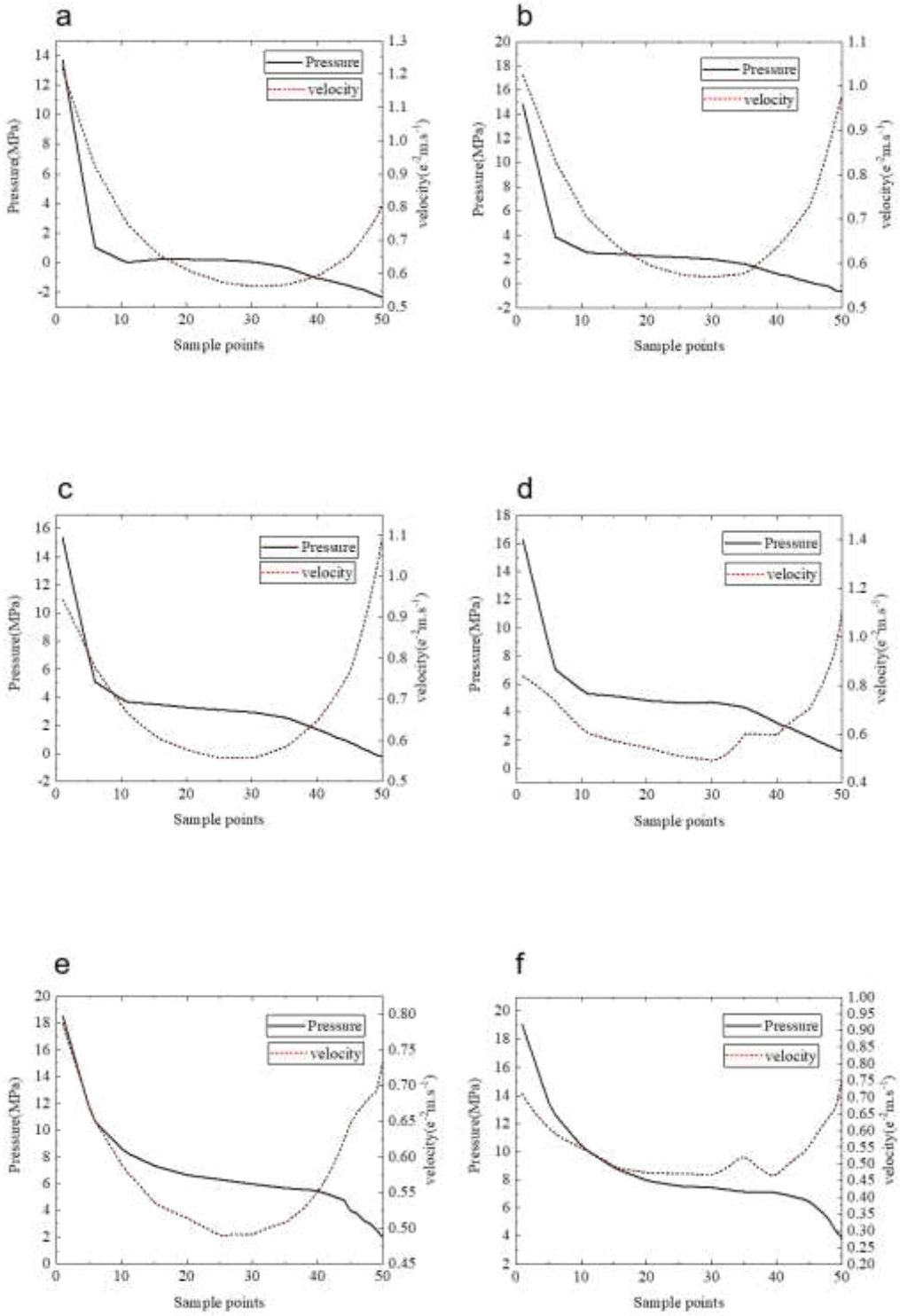
a
Pressure
velocity
Pressure(MPa)
velocity(e^{-2}m.s^{-1})
Sample points
b
Pressure
velocity
Pressure(MPa)
velocity(e^{-2}m.s^{-1})
Sample points
c
Pressure
velocity
Pressure(MPa)
velocity(e^{-2}m.s^{-1})
Sample points
d
Pressure
velocity
Pressure(MPa)
velocity(e^{-2}m.s^{-1})
Sample points
e
Pressure
velocity
Pressure(MPa)
velocity(e^{-2}m.s^{-1})
Sample points
f
Pressure
velocity
Pressure(MPa)
velocity(e^{-2}m.s^{-1})
Sample points

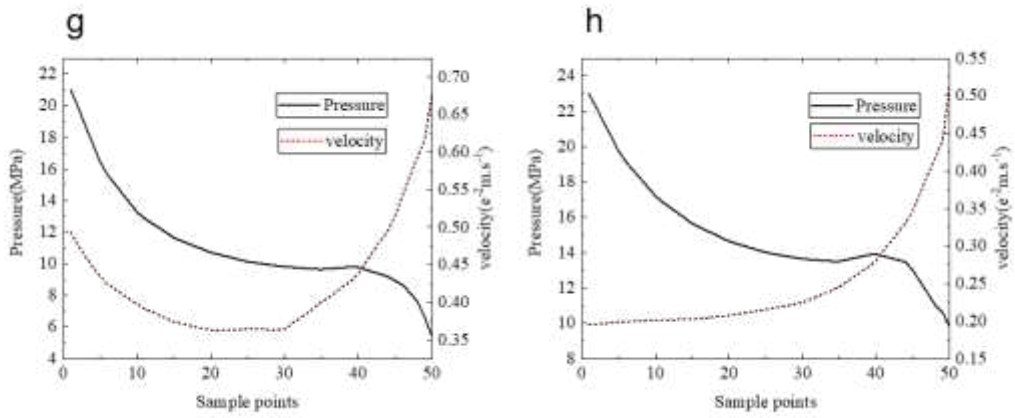

Figure 9 Variation of pressure and velocity distribution on raceway surface at different impact angles: (a)19°; (b)28°; (c)32°; (d)38°; (e)45°; (f)49°; (e)45°; (f)49°; (g)58°; (h)71°

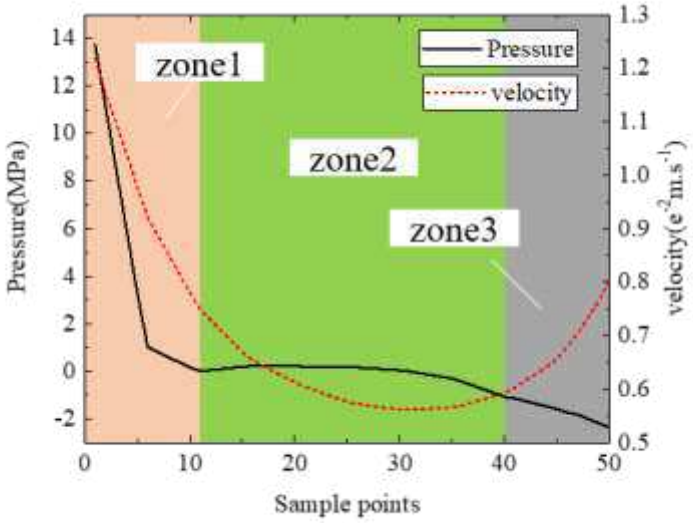

Figure 10 The evolution of pressure and velocity on raceway surface at 19° angle

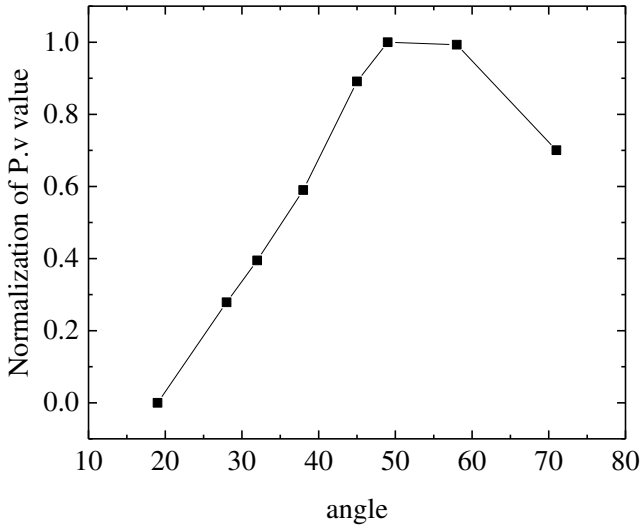

Figure 11 Normalization of P.v value at different impact angles

3.2. Evolution of surface roughness and MRR at different speeds

During the shear-thickening polishing process, the polishing speed is an important parameter that not only affects the shear rate, which in turn changes the dynamic viscosity but also affects the flow energy and boundary layer thickness of the slurry.

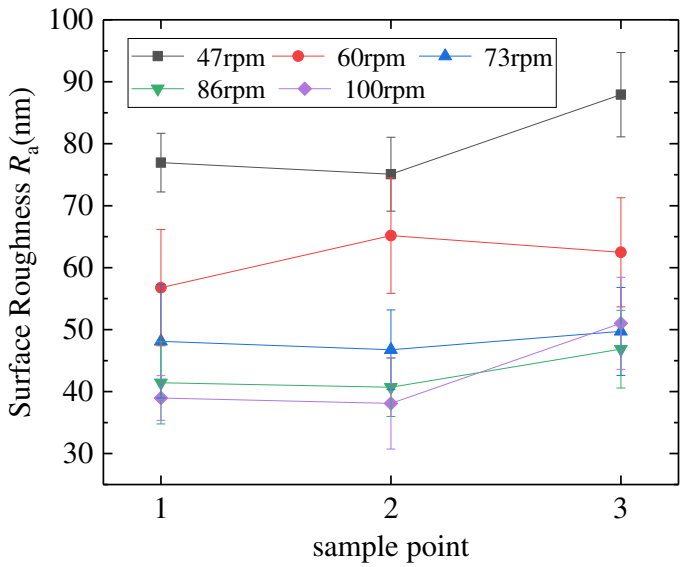

Figure 12 Surface roughness at different points after the STP

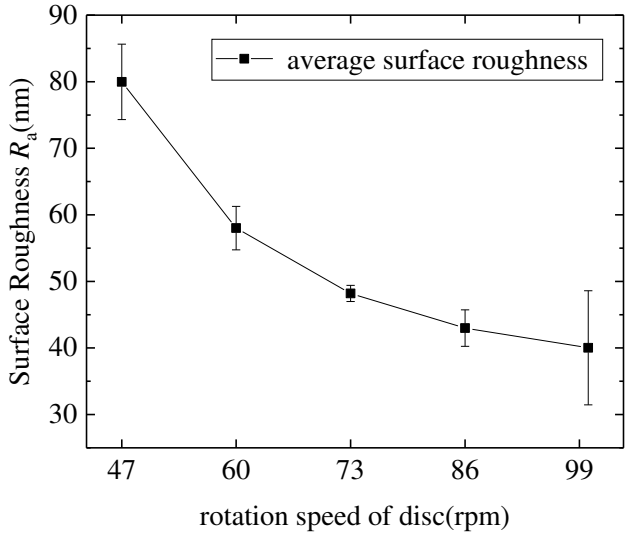

Figure 13 Average surface roughness after the STP with various rotation speed

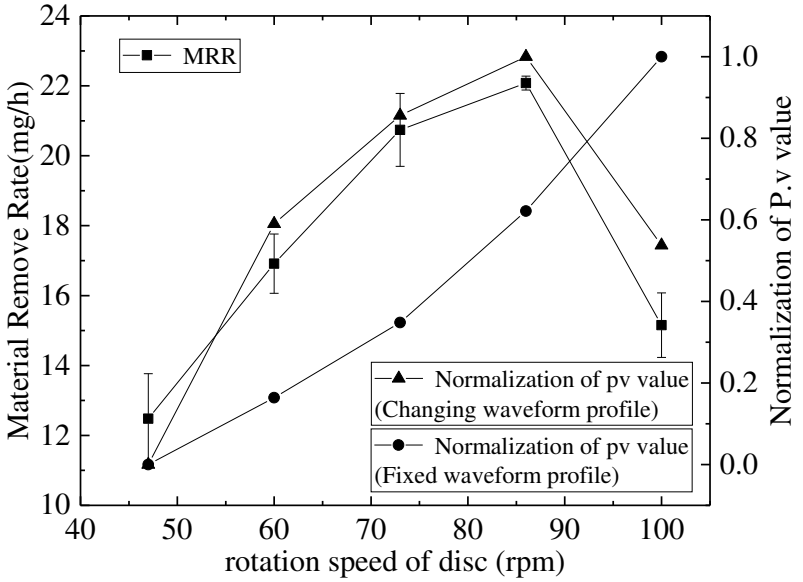

Figure 14 Comparison of experimental and simulated datum at different rotation speeds

Figure 12 and Figure 13 reveal that the surface roughness steadily decreases as impact velocity increases. The average surface roughness at points 1, 2, and 3 is found to be 79.9 nm at 47 rpm, which decreases steadily to 42.9 nm at 86 rpm. The average surface roughness was measured to be 40 nm at 100 rpm, which is the minimum value recorded in this experiment. However, it has the highest variance of 8.57 nm^2 at 100 rpm. This unusual finding suggests that the uniformity deteriorates at 100 rpm.

The variation of MRR for different rotation speeds of the disc is shown in Figure 14. The removal rate increases with increasing speed and attaining a maximum value of 22.08 mg/h at 86 rpm. Further increase in speed decreases the MRR to 15.15 mg/h at 100 rpm. The effect of speed on the polishing quality can be understood in three steps. Firstly, the theory of hydrodynamic flow

implies that the length of the inlet section of the pipe increases as the velocity increases, which leads to the smaller boundary layer thickness. Secondly, the higher velocity of shear-thickening slurry brings higher viscosity during the shear-thickening interval, which brings the improvement in removal efficiency. Lastly, the positive proportional relationship between the removal rate and P.v value has the greatest impact.

The phenomenon of rapid decrease in MRR with impact velocity at polishing rates of 86-100 rpm can be explained in two ways. The first is a result of changes in the waveform in the slurry flow channel, which results in variations in the impact angles. The second is the result of the abrasive particles experiencing greater centrifugal force at higher rotation speeds, resulting in fewer abrasive particles involved in the polishing process.

In order to understand the variation of MRR, simulation was performed to investigate the normalized datum of P.v value using the mathematical model established in the previous section (assuming that the change in polishing disc speed does not influence the waveform, and the value of impact angle is measured at 60 rpm). Another simulation was performed on the basis of true impact angles derived from polishing traces (waveform profile is changing). The results are shown in Figure 13, where the normalized P.v value and experiment datum have a highly consistent trend when considering angle change when comparing the MRR datum to the experimental datum. In contrast, the normalized equivalent of the P.v value linearly increases with the impact velocity with no change in the waveform. It is believed that the main factor causing the decrease of MRR at high rotation speed is the change of slurry profiles. Due to the uniform dispersion of slurry, the MRR value is almost independent of the centrifugal forces acting on the abrasive particles.

During the rotation, the slurry surface can be regarded as an equipotential surface. Neglecting the effect of internal friction, the sum of centrifugal potential energy and gravitational potential energy of slurry is assumed constant based on the principle of conservation of energy.

$$\begin{cases} E_c = \int_0^R -m\omega^2 r dr = -\dfrac{m\omega^2 R^2}{2} \\ E_g = mgz \\ E_c + E_g = const \\ z\,|_{R=0} = 0 \end{cases}$$

Where E_c is the centrifugal potential energy, E_g is the gravitational potential energy, and z is the height of the slurry surface. Solving the above system of equations, we can get the height of the slurry surface as: $z = \dfrac{\omega^2 R^2}{2g}$.

As shown in Figure 15, the waveform becomes steeper as the rotation speed increases and the contact area between the slurry and ring decreases, resulting in a lower MRR. It can be assumed that the MRR can be further improved if there is enough slurry in a large enough disc.

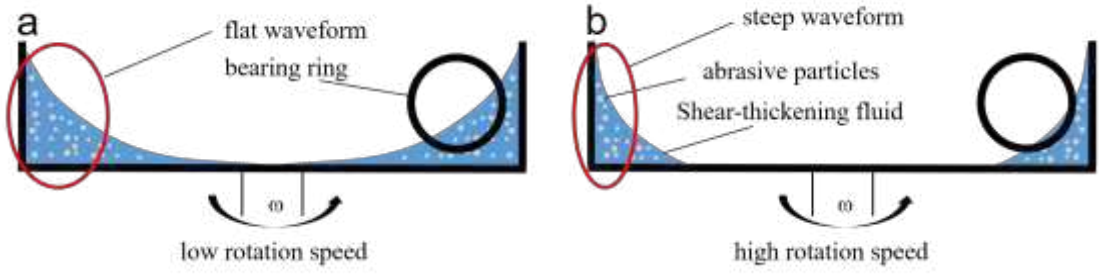

Figure 15 Waveforms of slurry at different rotational speeds, (a) low rotational speeds; (b) high rotational speeds

3.3 Edge effect of STP and design of guide block

3.3.1. The conception of edge effect and its causation

Surface roughness was measured at three points along the line of contact of the roller. If a measurement point 4 is added at the entrance of the ring (Figure 5) and is compared with the points 1-3 in terms of surface roughness, texture, and MRR after polishing, the machining efficiency of point 4 is much higher than that of point 1-3. The phenomenon of over-polishing at the entrance results in uneven polishing which is called the edge effect of STP.

In order to investigate the cause of the edge effect, the distribution of the P.v value along the flow direction of the slurry on the workpiece surface is simulated at different speeds. As shown in Figure 16, the P.v value at the entrance is much higher than that at the steady flow section, resulting in a rapid decrease of surface roughness at the entrance and higher processing efficiency. Although at different speeds, the P.v value starts falling at a distance of 2 mm along the axis.

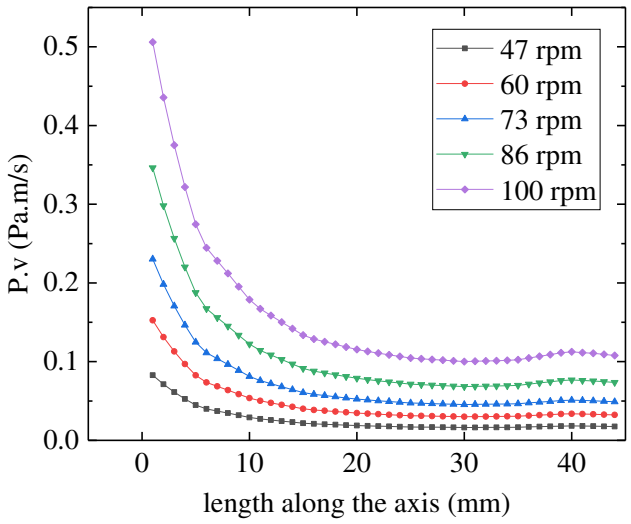

Figure 16 Variation of P.v value along the raceway surface

3.3.2. Guide block fixture and validation experiment:

Guide block is introduced in the fixture to realize the uniformity of STP. As shown in Figure 17, the guide block is set at the impact inlet of the slurry. The angle of the block is maintained at the same as that of the cross-section of the ring, while the length of the beveled edge is kept at 2 mm. A new measurement point 0 is added to the block, and point 1 is moved to the entrance.

The measured surface roughness after the application of STP with added guide block is shown in Figure 18. A notable difference in the surface roughness can be seen at different measuring points. The initial roughness of each point is around 310 nm. After 30 minutes of STP operation, the average roughness of points 1, 2, 3 dropped to 40 nm, while it was 17.87 nm at point 0. The overall datum is close to that obtained without guide blocks, which suggests that the block has little impact on the raceway surface. The surface roughness of point 0 decreases to 12.97 nm in 60 minutes and 5.77 nm in 90 minutes, while the corresponding values of average roughness for points 1, 2, 3 are 23.15

nm and 11.16 nm, respectively. The optical microscopic morphology of the raceway surface is shown in Figure 19 and Figure 20. The analysis showed that the variation in surface roughness of points 1, 2, and 3 is less than 0.58 nm^2, suggesting that the edge effect problem of STP was solved by sacrificing guide block, and hence STP provided a uniformly polished surface.

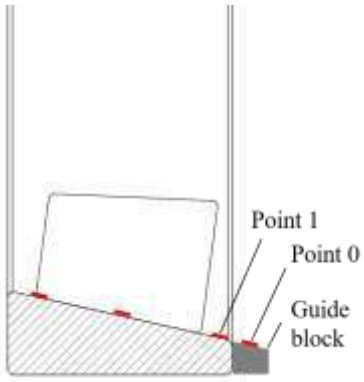

Figure 17 Guide block and new measurement points

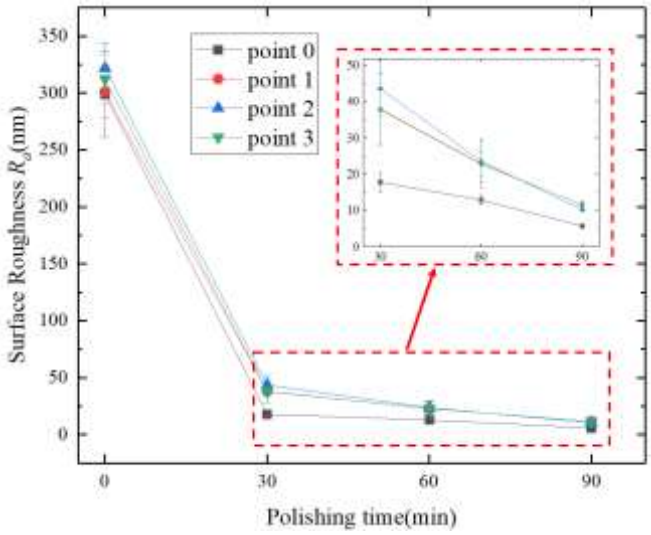

Figure 18 Evolution of different points over time

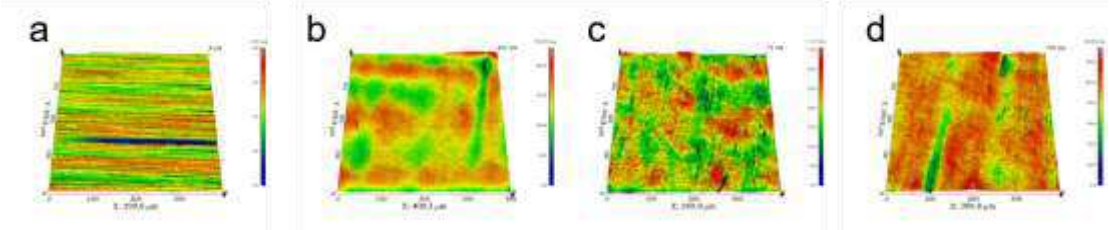

Figure 19 Surface morphology measured by optical 3D surface profiler : (a) initial surface morphology；(b) point 1；(c) point 2；(d) point 3

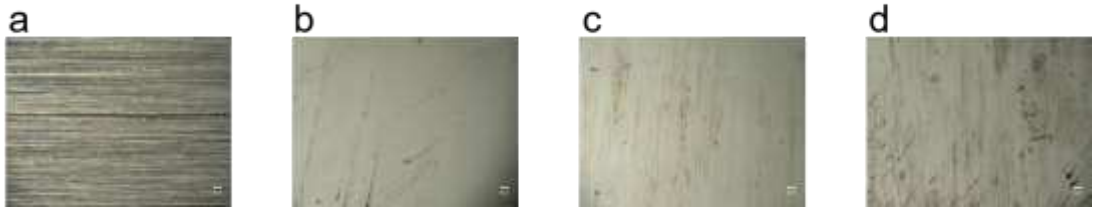

Figure 20 Surface morphology measured by a 3D microscope using a super-high magnification zoom lens: (a) initial surface morphology；(b) point 1；(c) point 2；(d) point 3

4. Conclusions

The shear-thickening polishing of the outer ring of 30203 bearing has been studied under varied inclination angles and slurry velocities. The optimal value of true impact angle was explored using a mathematical model and numerical analysis approach. Guide block was introduced to suppress the edge effect of the STP.

(1) The results show that impact angle has a significant influence on the polishing uniformity of the inner surface of the ring. The surface morphology observed significant changes at different inclination angles and the smoothest datum was found at 25° angle. The true impact angles derived from the mathematical model were found consistent with those in simulation data. The impact angle corresponding to the smoothest surface morphology was lying in the range of 45° to 65°.

(2) The highest MRR and lowest surface roughness were obtained at 86 rpm. This is due to the more pronounced shear-thickening properties of slurry and higher P.v value at higher rotational speeds. The MRR was further improved with a disc of large diameter and enough slurry.

(3) For the edge effect of STP, a guide block was introduced in the fixture to satisfy the uniformity requirement. After 90 minutes of the STP process, the average surface roughness R_a decreased from 310 nm to 11.16 nm, and the roughness variance was found under 0.58 nm^2.

This paper demonstrates the feasibility of STP for manufacturing the inner surface of a circular ring workpiece and can be used as a processing method to obtain an ultra-smooth inner surface.

Statement & declarations

Funding: The authors would like to thank the National Key R&D Program of China (No. 2018YFB2000400), National Natural Science Foundation of China (No.51805485, 51935008, 51905485, 52175442), Natural Science Foundation of Zhejiang Province (No.LY21E050010) for the financial support of this work. Also, the authors would like to thank the viewers for their feedback.

Completing Interests: We declare that we have no financial and personal relationships with other people or organizations that can inappropriately influence our work, there is no professional or other personal interest of any nature or kind in any product, service and/or company that could be construed as influencing the position presented in, or the review of, the manuscript entitled.

Availability of data and material: The authors confirm that the data and material supporting the findings of this study are available within the article.

Code availability: Not applicable.

Ethics approval: Not applicable.

Consent to participate: Not applicable.

Consent for publication: Not applicable.

Author contributions: Writing and analysis: Luguang Guo,Xu Wang; Experiments: Luguang Guo, Xu Wang, Yuechu Mao; CFD: Luguang Guo, Binghai Lyu; Data collection: Linlin Cao, Jinhu Wang; Surface roughness and morphology measurement: Hongyu Chen, Jiahuan Wang; Review: Julong Yuan.

References

[1] Zhang Z Y, Yan J W, T. K(2019). Manufacturing technologies toward extreme precision. International Journal of Extreme Manufacturing. 1:022001. https://doi.org/10.1088/2631-7990/ab1ff1

[2] Zhou T, He Y, Wang T, Zhu Z, Xu R, Yu Q, Zhao B, Zhao W, Liu P, Wang X(2021). A review of the techniques for the mold manufacturing of micro/nanostructures for precision glass molding. International Journal of Extreme Manufacturing. 3:042002. https://doi.org/10.1088/2631-7990/ac1159

[3] Wenhao L, Yan C, Rui Z, Liang X, Bing H(2021). Research process of remanufacturing technology. Diamond & Abrasive Engineering. 41:1-7. https://doi.org/10.13394/j.cnki.jgszz.2021.4.0001

[4] Chen H, Xu Q, Wang J, Li P, Yuan J, Lyu B, Wang J, Tokunaga K, Yao G, Luo L, Wu Y(2022). Effect of surface quality on hydrogen/helium irradiation behavior in tungsten. Nuclear Engineering and Technology https://doi.org/10.1016/j.net.2021.12.006

[5] He Z, Xie H, Zhong C, Wang Y, Zhang C, Deng D, An B, Liu Q, Yan F(2019). Influences of Lubrication Characteristics of Misaligned Sliding Bearings by Surface Roughness Models. Lubrication Engineering. 44:7-16.

[6] Zhao X, Sun J, Wang C, Wang H, Deng M(2013). Study on thermoelastohydrodynamic performance of bearing with surface roughness considering shaft deformation under load in shaft-bearing system. Industrial Lubrication And Tribology. 65:119-128. https://doi.org/10.1108/00368791311303483

[7] Hong G, Lanlan S, Shaolin Z, Weipei H(2020). Analysis of Static Characteristic of Hydrodynamic Bearing with Different Surface Roughnesses. Journal of Mechanical Transmission. 44:106-113. https://doi.org/10.1109/ICMTMA50254.2020.00011

[8] Romanowicz PJ, Szybiński B(2019). Fatigue Life Assessment of Rolling Bearings Made from AISI 52100 Bearing Steel. Materials. 12:371-392. https://doi.org/10.3390/ma12030371

[9] Nurul, rhana F, Mohd, Yusof, Zaidi, Mohd, Ripin(2014). Analysis of Surface Parameters and Vibration of Roller Bearing. Tribology Transactions. 57:715-729. https://doi.org/10.1080/10402004.2014.895887

[10] Grover V, Singh AK(2018). Improved magnetorheological honing process for nanofinishing of variable cylindrical internal surfaces. Materials And Manufacturing Processes. 33:1177-1187. https://doi.org/10.1080/10426914.2017.1339322

[11] Grover V, Singh AK(2019). Modeling of surface roughness in the magnetorheological cylindrical finishing process. Proc Inst Mech Eng Part E-J Process Mech Eng. 233:104-117. https://doi.org/10.1177/0954408917746354

[12] Grover V, Singh AK(2017). A novel magnetorheological honing process for nano-finishing of variable cylindrical internal surfaces. Materials And Manufacturing Processes. 32:573-580. https://doi.org/10.1080/10426914.2016.1257801

[13] Peng Z, Song WL, Ye CL, Shi P, Choi SB(2021). Model establishment of surface roughness and experimental investigation on magnetorheological finishing for polishing the internal surface of titanium alloy tubes. Journal of Intelligent Material Systems And Structures. 32:1278-1289. https://doi.org/10.1177/1045389x20930095

[14] Umehara N, Shibata I, Edamura K(1999). New polishing method with magnetic congelation liquid. Journal of Intelligent Material Systems And Structures. 10:620-623. https://doi.org/10.1106/t2jn-4ani-k7yf-rl3a

[15] Zhang L, He XS, Yang HR, Zhang Y(2010). An integrated tool for five-axis electrorheological fluid-assisted polishing. Int J Mach Tools Manuf. 50:737-740. https://doi.org/10.1016/j.ijmachtools.2010.04.003

[16] Zhang L, Kuriyagawa T, Kaku T, Zhao J(2005). Investigation into electrorheological fluid-assisted polishing. Int J Mach Tools Manuf. 45:1461-1467. https://doi.org/10.1016/j.ijmachtools.2005.01.021

[17] Zhang Z, Geng K, Qiao G, Zhang J(2021). The heat flow coupling effect of laser-assisted magnetorheological polishing. International Journal of Advanced Manufacturing Technology. 114:591-603. https://doi.org/10.1007/s00170-021-06880-3

[18] Wu LS, Zhang JY(2011). Study on Abrasive Flow Machining Pipe Inner Surface. International Conference on Textile Engineering and Materials (ICTEM 2011). Tianjin, PEOPLES R CHINA. 332-334:2014-2017. https://doi.org/10.4028/www.scientific.net/AMR.332-334.2014

[19] Zhang HY, Wu MY(2017). Polishing on Cubic Boron Nitride Abrasive Materials of Bearing Hollow Roller. Chinese Materials Conference (CMC). Yinchuan City, PEOPLES R CHINA.769-775. https://doi.org/10.1007/978-981-13-0107-0_74

[20] Zhao WH, Qu JY, Li JY, Su NN, Shi GF, Liu JH(2012). Research on quality analysis of solid-liquid two-phase abrasive flow precision machining based on different sub-grid scale models. The International Journal of Advanced Manufacturing Technology.14. https://doi.org/10.1007/s00170-021-07604-3

[21] Li J, Zhu J, Zhang H, Peng Q, Zhao W(2021). Vortex formation mechanism and experimental research of abrasive flow precision machining special inner curved surface based on large eddy simulation. The International Journal of Advanced Manufacturing Technology. 116:1-19. https://doi.org/10.1007/s00170-021-07537-x

[22] Wu MY, Gao H(2016). Experimental study on large size bearing ring raceways' precision polishing with abrasive flowing machine (AFM) method. The International Journal of Advanced Manufacturing Technology. 83:1927-1935. https://doi.org/10.1007/s00170-015-7706-x

[23] Li M, Lyu BH, Yuan JL, Dong CC, Dai WT(2015). Shear-thickening polishing method. Int J Mach Tools Manuf. 94:88-99. https://doi.org/10.1016/j.ijmachtools.2015.04.010

[24] Lyu B, Ke M, Fu L, Duan S, Shao Q, Zhou Y, Yuan J(2021). Experimental study on the brush tool-assisted shear-thickening polishing of cemented carbide insert. The International Journal of Advanced Manufacturing Technology. 115:2491-2504. https://doi.org/10.1007/s00170-021-07176-2

[25] Wang J, Lyu B, Jiang L, Shao Q, Deng C, Zhou Y, Wang J, Yuan J(2021). Chemistry enhanced shear thickening polishing of Ti-6Al-4V. Precision Engineering. 72:59-68. https://doi.org/10.1016/j.precisioneng.2021.04.002

[26] Song; Z, Lyu; B, Ke; M, Yang; Y, Shao; Q, Yuan; J, Nguyen D-n(2020). Removal rate model of deterministic shear thickening polishing material based on BP neural network. Surface Technology. 49:320-325,357. https://doi.org/10.16490/j.cnki.issn.1001-3660.2020.11.037

[27] Hu ZM, Dean TA(2000). A study of surface topography, friction and lubricants in metalforming. Int J Mach Tools Manuf. 40:1637-1649. https://doi.org/10.1016/S0890-6955(00)00014-6